# Model of Path-Dependent Plastic Instability

Asghar Zajkani, Ali Bandizaki

***Abstract—*** A model of path-dependent instability is developed for the substrate composite panels influenced by the non-linear reinforce elastomeric sheets. A modified maximum force (MMFC) is considered as well as the bifurcation criteria of vertex to predict diffuse and localized necking. By using a linear adoption of an equivalent strain the strain path effect are coupled. The quadratic Hill criterion is applied to analyze the anisotropy effect. Accuracy of the study is proved by comparing with the theoretical models.

***Keywords—*** Plastic instability, Diffuse and localized necking, Vertex model.

## I. INTRODUCTION

In a plastic stability model of deformation, the diffuse necking is started on the maximum value of the traction force. Swift used the results of Considèr studies for the biaxial tension [1]. Therefore, the model was called as the maximum force criterion (MFC). Hora et al. studied the diffuse necking phenomenon through investigations of the MFC model and experimental observations [2], [3]. The presented model by Hora et al. was so-called the Modified Maximum Force Criterion (MMFC). They claimed that the diffuse necking is strongly dependent on the strain hardening and the loading conditions. According to the MMFC, the diffuse necking in any loading conditions occurs in the plane strain conditions. The first study related to the localized necking was done by Hill for the uniaxial tension [4]. Alternately, Hill presented a zero extension for an evaluation of the necking band angle in the uniaxial tension [4]. There are some studies that use the Hill-Swift model to predict the necking [5]. Marciniak et al. investigated the localized necking through the experimental observations of the left-hand-side of the forming limit diagrams [6]. Stören and Rice [7] proposed a model based on the results extracted from previous works, in order to predict the localized necking on a homogeneous sheet. This model assumes that the velocity of the deformation is variable inside the necking band. Zajkani et al. proposed an analytical method to consider strain rate hardening on the vertex model by taking into account a dimensionless parameter under different conditions [8]. According to the Hill hypothesis, the angle is only dependent on the strain ratio. Therefore, for the state that the strain ratio is known (uniaxial tension ≤ strain ratio ≤ equi-biaxial tension) and the other stress ratios may be calculated from related constitutive formulations, the necking band angle would be dependent on the different parameters proposed by Zajkani et al. [9], [10]. They investigated a certain expression of the necking band angle, which provides the required accuracy of the results in comparison with the Hill zero extension. So, they named this angle by "dependent to yield criterion" or DYC-angle. Also, they studied the evolution of necking deformation in the strain rate dependent process [10]. Min et al. used a vertex model for predicting the LHS of the FLC's through the quadratic Hill yield criterion [11]. The studies by Hasford et al. show that the variations of the strain path can play an effective role in the FLD's results [12]. The pre-strain can occur at two major and minor directions of the loading. In considering the non-proportional loading, the both linear and especially non-linear paths are applied such as a finite element analysis reported in Ref. [13]. Chae et al. studied the strain path effect on the ductile fracture through the experimental and computational investigations [14]. Also, the numerical and experimental investigation of the non-linear strain path effect was studied by Larsson et al. [15]. The Hill-Swift model was used by Li et al. to study a bi-linear and non-linear strain path effects on the FLC's [16].

Here, the effect of reinforcing layers on a path-dependent plastic deformation in instability events considered. We also investigate the effects of both diffuse and localized necking. However, the MMFC model will be employed for the prediction of diffuse strains, but, for the localized necking, the vertex model will be used. Both models are considered in a delicate analytical way that has to be utilized for the experiments only through essential material constants. For the prediction of the necking band angle, the DYC-angle will be used to consider a dependency on the yield criterion, anisotropy, and the loading conditions. Since, the history of the loading is effective on the obtained limit strains, to evaluate the pre-strain effect on the diffuse and localized necking, both minor and major directions will be loaded under three conditions; i.e., the uniaxial, plane - strain and equi-biaxial pre-loadings. Also, the quadratic Hill yield criterion will describe the anisotropy effect on the path-dependent reinforced metal layer. The limit strains are obtained for the diffuse and localized necking in the elastomer-metal structures.

## II. BASIC FORMULATIONS

The substrate supported causes the retardation of plastic deformation by dissipating the absorbed energy and the improving the sheet surface quality. We employ the studies by Biot for describing the behavior of the neo-Hookean materials

Asghar Zajkani , Department of Mechanical Engineering, Imam Khomeini International University, Qazvin, Iran

Ali Bandizaki , Department of Mechanical Engineering, Imam Khomeini International University, Qazvin, Iran

https://doi.org/10.17758/EIRAI.F0118118

[17]. So, according to the Ref. [17], the strain energy is given by

$$Z = \frac{E}{6}(\lambda_1^2 + \lambda_2^2 + \lambda_3^2 - 3) \tag{1}$$

In (1), $E, \lambda$ are the elastic modulus and principal stretching related to the principal strains, respectively. Also, for the incompressible deformation, the strain energy is defined as follows

$$Z = \bar{\sigma}^s d\bar{\varepsilon} = \sigma_1^s d\varepsilon_1 + \sigma_2^s d\varepsilon_2 \tag{2}$$

Which, $\bar{\sigma}^s$ *and* $\bar{\varepsilon}$ are the equivalent stress and strain, respectively that the exponent*s* are related to the elastomer layer. These indexes 1 and 2 are related to the major and minor directions of the sheet, respectively. So, the stress field of the neo-Hookean reinforce layers can be obtained by combining differentiation of (1) and (2) as

$$\begin{aligned} \sigma_1^s &= \frac{\partial Z}{\partial \varepsilon_1} = \frac{E}{3}(\lambda_1^2 - \lambda_3^2) \\ \sigma_2^s &= \frac{\partial Z}{\partial \varepsilon_2} = \frac{E}{3}(\lambda_2^2 - \lambda_3^2) \end{aligned} \tag{3}$$

In (3), we have employed the plane stress and incompressible deformation assumptions $(\varepsilon_1 + \varepsilon_2 + \varepsilon_3 = 0)$. For the mentioned state, the principal stretching will be as the exponential functions as $\lambda_i = e^{\varepsilon_i}$. The time derivative of these strains and stresses are linked through instantaneous modules.

$$\sigma_{ij}^{J-s} = L_{ijkl}^s \left(\frac{\partial v_k}{\partial x_l}\right) \tag{4}$$

The instantaneous modules are symmetric.

Then, $L_{ijkl}^s = L_{jikl}^s = L_{ijlk}^s = L_{klij}^s$

$\sigma_{ij}^{J-s}$ is the Jaumann stress rate related to the elastomer layer. The stress rates are related to the Jaumann rate of the Cauchy stress that is as:

$$\sigma_{ij}^J = \dot{\sigma}_{ij} + W_{ni}\sigma_{nj} + \sigma_{in}W_{nj} \tag{5}$$

That the $W_{ni}$ is the spin tensor as

$$W_{ni} = \frac{1}{2}\left(\frac{\partial v_n}{\partial x_i} - \frac{\partial v_i}{\partial x_n}\right) \tag{6}$$

A plane – stress state is taken for the loading condition. We can say that there are only these principal stresses. Also, it is clear that $W_{ii} = 0$. By simplifying (6) into (5), we have:

$$\sigma_{11}^{J-s} = \dot{\sigma}_1^s = L_1^s\dot{\varepsilon}_1 + L_{12}^s\dot{\varepsilon}_2 \tag{7}$$
$$\sigma_{22}^{J-s} = \dot{\sigma}_2^s = L_2^s\dot{\varepsilon}_2 + L_{21}^s\dot{\varepsilon}_1 \tag{8}$$
$$\sigma_{12}^{J-s} = 2L_s^s\,\dot{\varepsilon}_{12} \tag{9}$$

According to (5) and the work in [17], the stresses rates are defined for the neo-Hookean reinforce layers in the plane stress conditions as

$$\begin{aligned} \dot{\sigma}_1^s &= \frac{4E}{9}\lambda_1^2\dot{\varepsilon}_1 - \frac{2E}{9}\lambda_2^2\dot{\varepsilon}_2 - \frac{2E}{9}\lambda_3^2\dot{\varepsilon}_3 + \dot{P} \\ \dot{\sigma}_2^s &= -\frac{2E}{9}\lambda_1^2\dot{\varepsilon}_1 + \frac{4E}{9}\lambda_2^2\dot{\varepsilon}_2 - \frac{2E}{9}\lambda_3^2\dot{\varepsilon}_3 + \dot{P} \\ \sigma_{12}^{J-s} &= \frac{E}{3}(\lambda_1^2 + \lambda_2^2)\dot{\varepsilon}_{12} \end{aligned}$$

where parameter $\dot{P}$ in the above relation is the rate of the hydrostatic stress as

$$\dot{P} = \frac{2E}{9}(\lambda_1^2\dot{\varepsilon}_1 + \lambda_2^2\dot{\varepsilon}_2 - 2\lambda_3^2\dot{\varepsilon}_3) \tag{11}$$

We will be able to obtain the instantaneous modulus

$$\begin{aligned} L_1^s &= \frac{2E}{3}(e^{2\varepsilon_1} + e^{2\varepsilon_3}) \\ L_2^s &= \frac{2E}{3}(e^{2\varepsilon_2} + e^{2\varepsilon_3}) \\ L_{12}^s &= L_{21s} = \frac{2E}{3}e^{2\varepsilon_3} \\ L_s^s &= \frac{E}{6}(e^{2\varepsilon_2} + e^{2\varepsilon_1}) \end{aligned} \tag{12}$$

## III. Path Dependency Formulation

For the non-proportional loading, the ratio of strain or the strain rate is different with the proportional loading. $\beta$ implies the strain ratio or strain rate ratio ( $\beta = \varepsilon_2/\varepsilon_1 = \dot{\varepsilon}_2/\dot{\varepsilon}_1$ ). The pre-power in related to the pre-strain parameters and the $i$ index is reagent the pre-straining direction. The equivalent strain is proposed with the linear assumption for considering the strain path effect.

$$\bar{\varepsilon} = \frac{1}{2}\left(\int_0^{\varepsilon_1^{pre}} \phi_i^{pre} d\varepsilon_1 + \int_{\varepsilon_1^{pre}}^{\varepsilon_1} \phi\, d\varepsilon_1 + \int_0^{\varepsilon_2^{pre}} \frac{\phi_i^{pre}}{\beta_1^{pre}}\, d\varepsilon_2 + \int_{\varepsilon_2^{pre}}^{\varepsilon_2} \frac{\phi}{\beta}\, d\varepsilon_2\right) \tag{13}$$

which,

$$\bar{\varepsilon} = \frac{1}{2}\left(\phi_i^{pre}\varepsilon_1^{pre} + \phi\,(\varepsilon_1 - \varepsilon_1^{pre}) + \frac{\phi_i^{pre}}{\beta_1^{pre}}\,\varepsilon_2^{pre} + \frac{\phi}{\beta}(\varepsilon_2 - \varepsilon_2^{pre})\right) \tag{14}$$

### A. *Pre-strained in the Major Direction*

The pre-strain ratio is as $\beta_1^{pre} = \varepsilon_2^{pre}/\varepsilon_1^{pre}$ and the index 1 is related to the major direction. The minor strain will be as

$$\varepsilon_2 = \int_0^{\varepsilon_1^{pre}} \beta_1^{pre}\, d\varepsilon_1 + \int_{\varepsilon_1^{pre}}^{\varepsilon_1} \beta\, d\varepsilon_1 = \beta_1^{pre}\,\varepsilon_1^{pre} + \beta\,(\varepsilon_1 - \varepsilon_1^{pre})$$

(1

Substituting the expression of $\beta_1^{pre} = \varepsilon_2^{pre}/\varepsilon_1^{pre}$ and (15) instead of the $\varepsilon_2^{pre}$ and $\varepsilon_2$ in the Eq. (23), respectively, we can obtain the equivalent strain for the pre-straining in the major direction in the following form

$$\bar{\varepsilon} = \phi_1^{pre}\varepsilon_1^{pre} + \phi\left(\varepsilon_1 - \varepsilon_1^{pre}\right) \quad (16$$

*B. Pre-strained in Minor Direction*

According to (13), the ratio of the strain will be determined as $\beta_2^{pre} = \varepsilon_1^{pre}/\varepsilon_2^{pre}$. The index of 2 is related to the minor direction. Subsequently, the ratio of the stresses and the strains related to the pre-straining will be changed. So, for this state, we can write $\alpha_2^{pre} = \sigma_1^{pre}/\sigma_2^{pre}$, $Q_2^{pre} = \bar{\sigma}^{pre}/\sigma_2^{pre}$, *and* $\phi_2^{pre} = \bar{\varepsilon}^{pre}/\varepsilon_2^{pre}$. Indeed, for the yield criterion ratios which are presented in Appendix, we may obtain $\alpha_2^{pre} = \alpha_1^{pre}, Q_2^{pre} = Q_1^{pre}$ *and* $\phi_2^{pre} = \phi_1^{pre}$, while $\beta_2^{pre} = 1/\beta_1^{pre}$. Accordingly, the minor strain will be obtained as

$$\int_{\varepsilon_2^{pre}}^{\varepsilon_2} d\varepsilon_2 = \int_{\varepsilon_1^{pre}}^{\varepsilon_1} \beta \, d\varepsilon_1 \quad (17$$

That

$$\varepsilon_2 = \varepsilon_2^{pre} + \beta(\varepsilon_1 - \beta_2^{pre}\varepsilon_2^{pre}) \quad (18)$$

By substituting (18) and the related expression of $\beta_2^{pre}$ instead of the $\varepsilon_2^{pre}$and $\varepsilon_2$, we can obtain an equivalent strain for the pre-staining at minor direction as

$$\bar{\varepsilon} = \left(\phi_2^{pre} - \beta_2^{pre}\,\phi\right)\varepsilon_2^{pre} + \phi\varepsilon_1 \quad (19)$$

## II. Modified maximum force criterion

Now, the effect of reinforce- layers on the MMFC is considered. According to the maximum force criterion assumption, the condition is satisfied for the multi-layer structure as following

$$dF_1 = d\sum_{i=1}^{N}(\sigma_1^i A_1^i\,) = 0 \quad (20)$$

By simplification and adopting an assumption of the incompressibility deformation, the above relation can be simplified as follows

$$t_s(-\sigma_1^s.\,d\varepsilon_1 + d\sigma_1^s) + t_m(-\sigma_1^m.\,d\varepsilon_1 + d\sigma_1^m) = 0$$

The $s, m$ powers are related to the elastomer substrate and the metal, respectively. For the cross-section, it is assumed as $A_1^s = b.t_s, A_1^m = b.t_m$ that this $b$, $t_i$ are related to the width and thickness of the sheet and reinforcing layer. The additional increment of the stress in the MMFC model can be expressed as

$$d\sigma_1 = \frac{\partial\sigma_1}{\partial\varepsilon_1}\,d\varepsilon_1 + \frac{\partial\sigma_1}{\partial\beta}\,d\beta \quad (22)$$

By substituting (21) into (22), the mathematical expression of the elastomer-metal structure can be determined in MMFC as

$$t_s\left(-\sigma_1^s + \frac{\partial\sigma_1^s}{\partial\beta}\frac{\partial\beta}{\partial\varepsilon_1}\right) - t_m\left(\sigma_1^m - \frac{\partial\sigma_1^m}{\partial\varepsilon_1} - \frac{\partial\sigma_1^m}{\partial\beta}\frac{\partial\beta}{\partial\varepsilon_1}\right) = 0 \quad (23$$

The term of $\partial\sigma_1/\partial\varepsilon_1$ in the MMFC is related to the strain hardening effect and the $(\partial\sigma_1/\partial\beta).(\partial\beta/\partial\varepsilon_1)$ expresses the variation of the loading condition. In the elastomer, the strain hardening can be negligible. The $\sigma_1^s$ has been presented in (3), while quantity of $\sigma_1^m$ will be evaluated by employing the power-low strain hardening as $\bar{\sigma} = k\bar{\varepsilon}^n$. By using the strain hardening, the second term of (23) related to the metal layer can be obtained as follows

$$\frac{\partial\sigma_1^m}{\partial\varepsilon_1} = \frac{\partial\sigma_1^m}{\partial\bar{\sigma}}\frac{\partial\bar{\sigma}}{\partial\bar{\varepsilon}}\frac{\partial\bar{\varepsilon}}{\partial\varepsilon_1} = \phi^2 E_t \quad (24)$$

$E_t$ is the tangent module. The third term of (24) related to the metal layer is expanded as

$$\frac{\partial\sigma_1^m}{\partial\beta} = \frac{\partial}{\partial\alpha}\left(\frac{\bar{\sigma}}{Q}\right)\frac{\partial\alpha}{\partial\beta} = -\frac{\bar{\sigma}}{Q^2}\frac{\partial\alpha}{\partial\beta}\frac{\partial Q}{\partial\alpha} \quad (25$$

Also, by using (3) related to the elastomer, we can write

$$\frac{\partial\sigma_1^s}{\partial\beta} = -\frac{\sigma_1^s}{Q}\frac{\partial\alpha}{\partial\beta}\frac{\partial Q}{\partial\alpha} \quad (26)$$

The effect of materials and thickness ratio of the elastomer-metal structure is defined using a parameter of $\omega = (Et_s)/(kt_m)$. In considering the strain path effect on the diffuse necking, it should be used the equivalent strain and the strain ratio related to the pre-straining direction. For this purpose, it's assumed that the elastomer substrate is applied to the metal layer before pre-straining and so, the metal-elastomer structure is being included the history of the loading. We have

- pre − straining in major direction:

$$\frac{\partial\beta}{\partial\varepsilon_1} = -\frac{\left(\varepsilon_2 - \beta_1^{pre}\varepsilon_1^{pre}\right)}{\left(\varepsilon_1 - \varepsilon_1^{pre}\right)^2} = \frac{-\beta}{\varepsilon_1 - \varepsilon_1^{pre}} \quad (27)$$

- pre − straining in minor direction:

$$\frac{\partial\beta}{\partial\varepsilon_1} = -\frac{\left(\varepsilon_2 - \varepsilon_2^{pre}\right)}{\left(\varepsilon_1 - \beta_2^{pre}\varepsilon_2^{pre}\right)^2} = \frac{-\beta}{\varepsilon_1 - \beta_2^{pre}\varepsilon_2^{pre}} \quad (28$$

Difference between experiments and theoretical results are shown in Fig. (1). In the RHS of the FLD's. In this study, the term is assumed one. This subject is in effect the different effect of stress triaxiality on the materials. The Fig. (1) shows that the $\partial\beta/\partial\varepsilon_1$ has more drastic role on the RHS of the

FLD's. Substituting the corresponding equivalent strain, the final equation of the diffuse necking will be obtained per the elastomer-metal structures pre-strained.

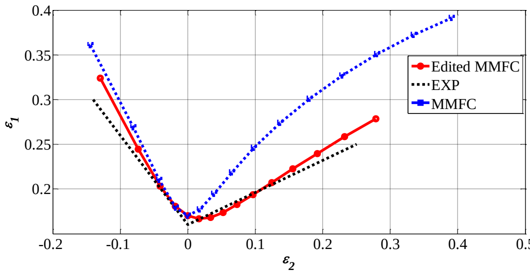


Fig. 1: The edited MMFC and MMFC and experimental DC01 steel sheet [18]

The pre-strain can be in the $-0.5 \le \beta_i^{pre} \le 1$ range. The $\omega = 0$ is related to freestanding metal layer, and if the pre-strain component is zero, the equation will be decreased to the simple MMFC, which those related equations are linear for the mentioned conditions.

## III. VERTEX MODEL

However, the vertex model predicts the localized necking as the nominal stress rate being zero in the localized necking band [7], it's clear that the strains are approximately regarded equal to the diffusion necking around of the localized band. So, for the velocity of deformation, we can write

$$\begin{aligned}\Delta v_i = v_{i,\text{localized}} - v_{i,\text{diffusion}} \\ = v_{i,\text{inside}} - v_{i,\text{outside}}\end{aligned} \quad (29)$$

According to the Stören and Rice studies, the rate of the plastic deformation is discontinuous in the localized necking band [7]. So, for the variations of the deformation velocity by employing the Green transformation can be written as

$$\iiint_{\forall} \nabla_j.(\Delta v_i)\, d\forall = \oint\!\!\oint_A g_i' n_j\, dA = g_i\, n_j \quad (30$$

In above relation, the $\nabla_j$ is the gradient by $j$ and the $g_i$ is the function of the Eulerian place and time. Also, the $n_j$ is the normal vector as $n_1 = \cos\theta$ *and* $n_2 = \sin\theta$. The discontinuity of the deformation rate in the necking band is while the stress and strain are continuous [7]. The rate of the Eulerian deformation tensor is characterized the strain rate tensor that is a symmetric tensor.

$$\Delta\dot{\varepsilon}_{ij} = \frac{1}{2}\left(\Delta v_{i,j} + \Delta v_{j,i}\right) = \frac{1}{2}\left(g_i\, n_j + g_j\, n_i\right) \quad (31)$$

The general form of the force equilibrium equation is as

$$\nabla_i.(\sigma_{ii} t) + \nabla_j.\left(\sigma_{ij} t\right) = 0 \quad (32)$$

But, develop of the deformation can be caused the rotation and create the shear stress. Indeed, it's possible that the tension loading doesn't stay in the principal directions. This subject is investigated by Zhu et al. in a minimal element and found that the shear stress terms vanished [19]. So, by using the Green transformation and the incompressible plastic deformation assumption the modified time derivative equilibrium equation for the plane stress condition can be as

$$\begin{cases}\Delta\dot{\sigma}_1 - \sigma_1(g_1 n_1 + g_2 n_2) = 0 \\ \Delta\dot{\sigma}_2 - \sigma_2(g_1 n_1 + g_2 n_2) = 0\end{cases} \quad (33$$

The related objective time derivative stress is the Jaumann stress rate of the Cauchy stress. The objectivity of the stress rates on the vertex theory is investigated in Ref. [9]. According to the Hill assumption, the variations of the shear strain rate are zero [4]. So,

$$\Delta\dot{\varepsilon}_{12} = \frac{1}{2}(g_1\, n_2 + g_2\, n_1) = 0 \quad (34$$

As previously mentioned, according to Zhu et al. the rate of the shear stress is zero [19]. In the state that the $\beta$ is input for calculating the $\alpha$, the necking band angle is dependent on the yield criterion and the related parameter as anisotropy. The details about the DYC-angle and comparing the effects of the yield criterion are presented in Refs. [10], [9]. According to the Ref. [10], the equi-biaxial loading is independent of the necking band angle. They showed that the DYC-angle presenting better FLD's results in comparison with the Hill zero extension. The relation between the rates of the stress and strain is presented in (4). The instantaneous module for the metal layer is as

$$\begin{aligned}L_{ijkl}^m = \frac{2}{3}\, E_s \left[\frac{1}{2}\left(\delta_{ik}\delta_{jl} + \delta_{jk}\delta_{il}\right) - \frac{1}{3}\delta_{ij}\delta_{kl}\right] \\ - (E_s - E_t)\frac{\sigma_{ij}\sigma_{kl}}{\sigma_e^2} + C_{ijkl}^m\end{aligned} \quad (35$$

By using the related values, we have

$$L_{11}^m = E_s\left[\frac{4}{3} - (1-n)\left(\frac{1}{Q}\right)^2\right] \quad (36)$$

$$L_{22}^m = E_s\left[\frac{4}{3} - (1-n)\left(\frac{\alpha}{Q}\right)^2\right] \quad (37)$$

$$L_{12}^m = L_{21}^m = E_s\left[\frac{2}{3} - (1-n)\frac{\alpha}{Q^2}\right] \quad (38)$$

The bifurcation analysis of the elastomer-metal structure that are under tension be done by investigation the satisfying the localized necking conditions. For this purpose, the difference between the nominal stress rates on the inside and outside of the necking band in the vertex model must be zero. So

$$t_m.\Delta\dot{T}_{ij}^m + t_s.\Delta\dot{T}_{ij}^s = 0 \quad (39)$$

$\Delta\dot{T}_{ij}^m$ and $\Delta\dot{T}_{ij}^s$ are the variations of the nominal stress rate related to the metal and elastomer, respectively.

$$\Delta\dot{T}_{ij} = n_i\left(\sigma_{ij}^J + \sigma_{in}.\Delta v_{j,n} - \left(\sigma_{in}.\dot{\varepsilon}_{jn} + \sigma_{jn}.\dot{\varepsilon}_{in}\right)\right) \quad (40)$$

The above equation is a non-linear equation of the $\boldsymbol{g}$ *and* $\boldsymbol{\varepsilon}$ roots. Finally, the final equation of the elastomer-metal structure will be obtained by taking into account the coefficient of determinant of the following matrix:

$$\begin{bmatrix} G_{11} & G_{12} \\ G_{21} & G_{22} \end{bmatrix} \begin{bmatrix} g_1 \\ g_2 \end{bmatrix} = 0 \qquad (41)$$

## IV. RESULTS AND DISCUSSION

The MMFC model is edited for improving the RHS of the FLD’s. Also, for the localized necking band, the DYC-angle considering the dependency of the angle to the yield criterion is used. The effect of pre-straining is proposed in the equations as a linear strain path and is studied for both major and minor directions in any three mentioned conditions and compared with the experimental results. The results of the MMFC are validated with the experimental results in Ref. [12]. Then, the effect of the pre-straining on the substrate supported metal layer is investigated.

The Fig. (2) shows the effect of the uniaxial pre-straining in the major direction on the MMFC model. According to this illustration, the domain of minor strain is shrunk with the increase of the uniaxial loading history. On the other hand, the increase of uniaxial pre-straining in the major direction causes the moving the FLC's to the left side of the FLD’s. It is showing that the major strain in the plane - strain condition will be obtained in higher values with the increase the uniaxial pre-straining. But, according to Fig. (3), the minor strain becomes zero in any pre-straining at the plane strain condition in the major direction. The domain of the minor strain in the plane strain pre-straining is the same of the uniaxial pre-straining influence as an increase of the pre-strain values leads to descending this domain. In the equi-biaxial case that pre-straining is equal in both directions, the Fig. (3) presents the corresponding results in which movement of the pre-strained FLC's into the RHS of the FLD'S can be observable. Accordingly, the major strain in the plane strain condition is smaller than the as-received in equi-biaxial pre-strained. Subsequently, in a general comparison, the equi-biaxial pre-straining is independent of the strain path direction, and it is caused the shrink of the forming limit. In comparison the effect of strain path on the FLD's in uniaxial and plane strain pre-loading we can say, the uniaxial pre-straining is more efficient on the major strains. But, in the plane strain conditions, the plane strain pre-loading has better results.

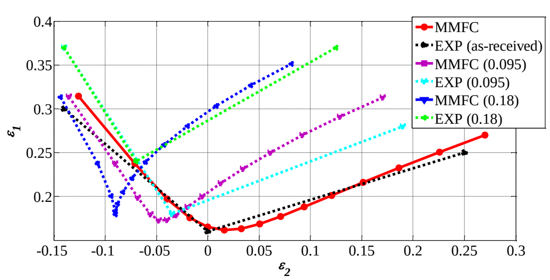


Fig. 2: Comparison of the experiment and MMFC results in the uniaxial pre-straining at the major direction

But, in all three pre-straining conditions, it is observed that it decreased the minor strain domains. The presented results in Fig (4) and Fig (5) relate to the minor direction of pre-straining. It is clear that the effect of pre-straining direction is very active on the FLC's. The loading history has different rules in any pre-loading directions. As the increase of the pre-strain value in the minor direction is causes the moving of the related FLC’s to the RHS and down part of the as-received FLD. In the non-proportional loading of the MMFC results, it is shown that the direction of the pre-loading can be effective to the limit of the necking instability. While the pre-straining in the major direction leads to increase the limit strains at the major direction, it causes the decrease of the limit strains when the pre-straining is taken place in the minor direction.

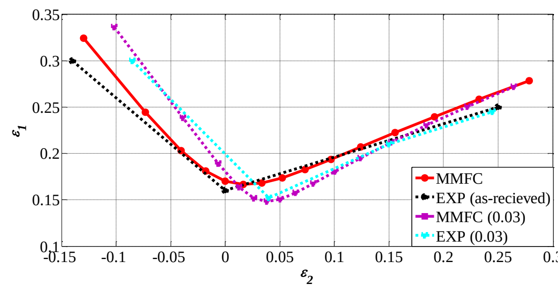


Fig.3: Comparison of the experiment and MMFC results in the equi-biaxial pre-straining

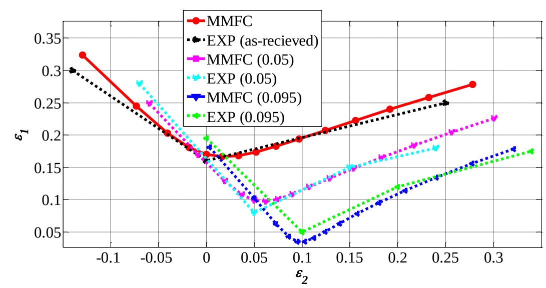


Fig.4: Comparison of the experiment and MMFC results in the Uniaxial pre-straining at the minor direction

Of course, the mentioned point is related to the uniaxial and plane strain conditions. For the equi-biaxial pre-straining, the domain of the minor strains is decreased.

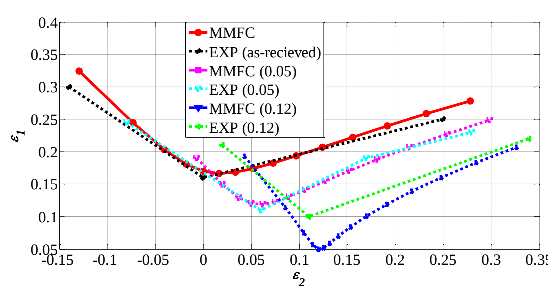


Fig.5: Comparison of the experiment and MMFC results in the plane strain pre-straining at the minor direction

Also, the increase the pre-straining value, lead to shrinking the major limit strains. But, the minor strains in the RHS of

https://doi.org/10.17758/EIRAI.F0118118

the FLD's are increased with the enhancement of the pre-straining. In a general discussion about the non-proportional loading of diffuse necking, the major pre-straining can be useful in the increase of the formability in the major strains. But, the domains of the minor strains will be decreased. The uniaxial pre-strained in major direction has the best result in the main strains. But, the pre-strained in the major direction for the plane strain condition, including the best results for the plane strain conditions, while the pre-straining in the minor direction reduces the formability. Indeed, the behavior of the materials in pre-strained in these major and minor directions are fully reversible.

## References


[1] H. W. Swift, "Plastic instability under plane stress," J. Mech. Phys. Solids, vol. 1, no. 1, pp. 1–18, 1952.
https://doi.org/10.1016/0022-5096(52)90002-1

[2] P. Hora, L. Tong, and B. Berisha, "Modified maximum force criterion, a model for the theoretical prediction of forming limit curves," Int. J. Mater. Form., vol. 6, no. 2, pp. 267–279, 2013.
https://doi.org/10.1007/s12289-011-1084-1

[3] Hora P. Tong L, "Prediction methods for ductile sheet metal failure using FE-simulation," InProc. IDDRG Congr., pp. 363–375, 1994.

[4] F. Abed-Meraim, T. Balan, and G. Altmeyer, "Investigation and comparative analysis of plastic instability criteria: Application to forming limit diagrams," Int. J. Adv. Manuf. Technol., 2014.
https://doi.org/10.1007/s00170-013-5530-8

[5] R. Hill, "On discontinuous reference plastic states , with special to localized necking in thin sheets," J. Mech. Phys. Solids, vol. 1, pp. 19–30, 1952.
https://doi.org/10.1016/0022-5096(52)90003-3

[6] Z. Marciniak, K. Kuczyi, and S. K. I. Warsaw, "Limit strains in the processes of stretch-forming sheet metal," Int. J. Mech. Sci., vol. 9, pp. 609–620, 1967.
https://doi.org/10.1016/0020-7403(67)90066-5

[7] S. Stören and J. R. Rice, "Localized necking in thin sheets," J. Mech. Phys. Solids, vol. 23, no. 6, pp. 421–441, 1975.
https://doi.org/10.1016/0022-5096(75)90004-6

[8] [8] A. Zajkani, A. Bandizaki, "A rate and stress dependent modeling of necking onset in metallic sheets based on Vertex plastic instability."

[9] A. Zajkani A . Bandizaki "A plastic instability analysis of the substrate reinforced sheet metals based on the localized Vertex theory of forming limit."

[10] A. Zajkani, A . Bandizaki "An efficient model for diffuse to localized necking transition in rate-dependent bifurcation analysis of metallic sheets,"submitted in Int. J. Mech. Sci. 2017
https://doi.org/10.1016/j.ijmecsci.2017.09.054

[11] J. Min, J. Lin, Y. Cao, W. Bao, and Z. Lu, "Effect of necking types of sheet metal on the left-hand side of forming limit diagram," J. Mater. Process. Technol., vol. 210, no. 8, pp. 1070–1075, 2010.
https://doi.org/10.1016/j.jmatprotec.2010.02.018

[12] A. Graf and W. Hasford, "The influence of strain-path changes on forming limit diagrams of a1 6111 t4," Int. J. Mech. Sci, vol. 36, no. 10, pp. 897–910, 1994.
https://doi.org/10.1016/0020-7403(94)90053-1

[13] W. Volk, H. Hoffmann, J. Suh, and J. Kim, "Failure prediction for nonlinear strain paths in sheet metal forming," CIRP Ann. - Manuf. Technol., vol. 61, no. 1, pp. 259–262, 2012.
https://doi.org/10.1016/j.cirp.2012.03.111

[14] D. Chae, J. . Bandstra, D. . Koss, C. D., B. J.P., and K. D.A., "The effect of pre-strain and strain-path changes on ductile fracture: experiment and computational modeling," Mater. Sci. Eng. A, vol. 285, no. 1–2, pp. 165–171, 2000.
https://doi.org/10.1016/S0921-5093(00)00642-0

[15] R. Larsson, O. Björklund, L. Nilsson, and K. Simonsson, "A study of high strength steels undergoing non-linear strain paths - Experiments and modelling," J. Mater. Process. Technol., vol. 211, no. 1, pp. 122–132, 2011.
https://doi.org/10.1016/j.jmatprotec.2010.09.004

[16] H. Li, G. Li, G. Gao, W. Zhang, and X. Wu, "A formability evaluation method for sheet metal forming with non-linear strain path change," Int. J. Mater. Form., pp. 1–13, 2017.
https://doi.org/10.1007/s12289-017-1342-y

[17] M. A. Biot, Mechanics of Incremental Deformation: Theory of Elasticity and Viscoelasticity of Initially Stressed Solids and Fluids, Including Thermodynamic Foundations and Applications to Finite Strain. 1965.
https://doi.org/10.1063/1.3047001

[18] D. S. Comsa, G. Dragos, L. Paraianu, and D. Banabic, "Prediction of the Forming Limit Band for Steel Sheets using a new Formulation of Hora ' s Criterion ( MMFC )," pp. 425–431, 2010.

[19] X. Zhu, K. Weinmann, and A. Chandra, "A Unified Bifurcation Analysis of Sheet Metal Forming Limits," J. Eng. Mater. Technol., vol. 123, no. 3, p. 329, 2001
https://doi.org/10.1115/1.1370397